The Astrophysical Journal, 656:444–455, 2007 February 10

SPITZER IRS SPECTROSCOPY OF INTERMEDIATE POLARS: CONSTRAINTS ON MID-INFRARED CYCLOTRON EMISSION

Thomas E. Harrison[1] and Ryan K. Campbell[1]
Department of Astronomy, New Mexico State University, Las Cruces, NM; tharriso@nmsu.edu, cryan@nmsu.edu

Steve B. Howell
WIYN Observatory and National Optical Astronomy Observatories, Tucson, AZ; howell@noao.edu

France A. Cordova
Institute of Geophysics and Planetary Physics, Department of Physics,
University of California, Riverside, CA; france.cordova@ucr.edu

and

Axel D. Schwope
Astrophysikalisches Institut Potsdam, Potsdam, Germany; aschwope@aip.de
Received 2006 September 29; accepted 2006 November 1

ABSTRACT

We present *Spitzer* IRS observations of 11 intermediate polars (IPs). Spectra covering the wavelength range from 5.2 to 14 μm are presented for all 11 objects, and longer wavelength spectra are presented for three objects (AE Aqr, EX Hya, and V1223 Sgr). We also present new, moderate-resolution ($R \sim 2000$) near-infrared spectra for five of the program objects. We find that, in general, the mid-infrared spectra are consistent with simple power laws that extend from the optical into the mid-infrared. There is no evidence for discrete cyclotron emission features in the near- or mid-infrared spectra for any of the IPs investigated, nor for infrared excesses at $\lambda \leq 12$ μm. However, AE Aqr, and possibly EX Hya and V1223 Sgr, do show longer wavelength excesses. We have used a cyclotron modeling code to put limits on the amount of such emission for magnetic field strengths of $1 \leq B \leq 7$ MG. If cyclotron emission is occurring in the 5.2–14.0 μm bandpass, it constitutes less than 1% of the bolometric luminosity of *any* of the IPs. We were able to model the long-wavelength excess of V1223 Sgr and EX Hya with cyclotron emission from a 1 MG field, but the S/N of those data is very poor, and the reality of those excesses is not established. We attempted to model the long-wavelength excess of AE Aqr with cyclotron emission, but none of our models fit nearly as well as a simple, cool ($T_{\rm BB} = 140$ K) blackbody. Given the apparent variability of this excess, however, synchrotron radiation remains a better explanation. We discuss our results in the context of the standard model for IPs.

Subject headings: infrared: stars — stars: individual (AE Aquarii, AO Piscus, DQ Herculis, EX Hydrae, FO Aquarii, GK Persei, PQ Geminorum, TV Columbae, TX Columbae, V603 Aquilae, V1223 Sagitarii)

1. INTRODUCTION

Intermediate polars (IPs) are a subclass of cataclysmic variable that are believed to harbor magnetic white dwarf primaries that are accreting matter from low-mass, late-type secondary stars. They are identified by a combination of multiperiodic photometric behavior and hard X-ray spectra (see Warner 1995). They differ from the "polars" in that the magnetic field strength of the primary is believed to be weaker, based on the lack of detectable polarization or discrete cyclotron harmonics in their optical/near-infrared spectra. Also, in contrast to polars, the white dwarf primaries in IPs are rotating asynchronously with periods that are substantially shorter than the orbital period of the binary. Instead of capturing the accretion stream close to the secondary star and funneling it onto the magnetic poles, a truncated accretion disk appears to be present in most IPs, the inner edge of which is then captured by the magnetic field of the white dwarf, although "stream-fed" systems are believed to exist (e.g., Norton et al. 2004a).

The rapid rotation of the white dwarf creates a magnetosphere, inside of which the accreted matter flows along the field lines and accretes onto the primary after passing through a shock. The shock is the source of the X-ray emission, and the spin rates of the white dwarfs in many IPs have been discovered using X-ray observations. Due to the possibility of either gaining or losing angular momentum through the interaction of the magnetic field with the accreting matter, the white dwarfs in IPs could be either spun-up (e.g., AO Psc; van Amerongen et al. 1985) or spun-down (e.g., V1223 Sgr; van Amerongen et al. 1987). But Norton et al. (2004b) show that there is a large range of parameter space that allows for rotational equilibrium.

In the synchronously rotating polars, the accretion process is simpler, and as the material approaches the white dwarf primary, a hot shock forms, emitting X-rays. Depending on the accretion rate, cyclotron emission can be the dominant cooling process. During periods of relatively low-mass accretion rates, strong, discrete cyclotron harmonics are observed in optical and/or infrared spectra of polars (Fig. 1), that can lead to robust estimates of the magnetic field strength and allow for estimations of the conditions in the accretion column. The presence of X-ray emission and, in a few cases, circularly polarized light, suggests that magnetically controlled accretion *is* occurring in IPs. However, most IPs do not show any sign of polarization, and no IP has ever displayed discrete cyclotron emission humps. Thus, a standard model has been constructed that assumes that the field strength of

[1] Visiting Astronomer at the Infrared Telescope Facility, which is operated by the University of Hawaii under contract from the National Aeronautics and Space Administration.

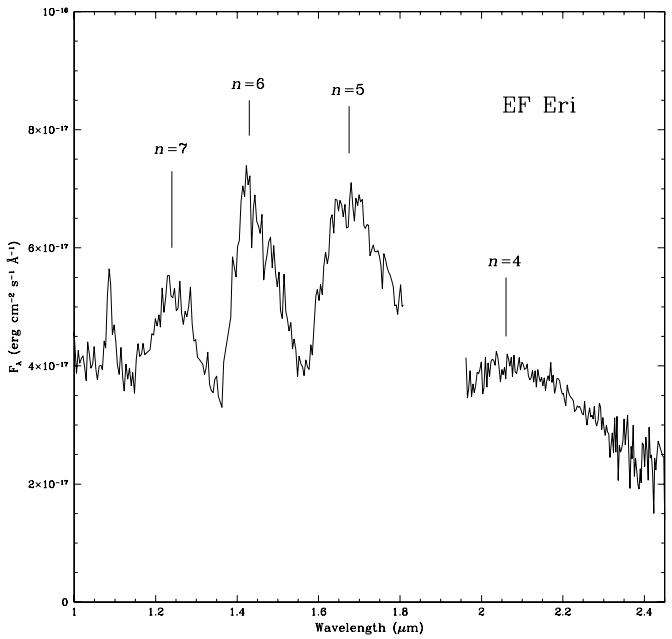

FIG. 1.— SPEX low-resolution spectrum of EF Eri showing cyclotron emission from the $n = 5$, 6, and 7 harmonics from a 13.6 MG field in the J and H bands. The $n = 4$ harmonic from this field falls in the K band and is partially optically thick. Emission from He I (+H I Paγ) at 1.083 μm is clearly present.

the magnetic white dwarf primary must be lower than $B \leq 8$ MG, and that the accretion rates in IPs are higher than those in polars. Wickramasinghe et al. (1991) show that this model is consistent with the observational data for IPs.

Due to higher accretion rates, discrete cyclotron emission is suppressed, and any circular polarization from the higher harmonics is highly diluted by the flux from the disk. Thus, to search for the cyclotron emission from IPs, observations at mid-infrared wavelengths are necessary. At wavelengths longer than 2 μm, the cyclotron emission should be detectable for fields with $B \leq 10$ MG even in the presence of strong disk emission. Since mid-infrared polarization is not yet feasible for such faint sources, detection of excess emission using mid-infrared spectroscopy may be our only method for confirming this model and estimating field strengths, and accretion parameters in IPs.

We present a mid-infrared spectroscopic survey of 11 IPs obtained using the Infrared Spectrograph (IRS) on the *Spitzer Space Telescope*. We find no evidence for cyclotron emission at wavelengths below 12 μm, and in general the IRS spectra are consistent with a simple power-law form extrapolated from the optical and near-infrared into the mid-infrared. We do find a significant excess at $\lambda > 12$ μm for AE Aqr, but conclude that it is also not due to cyclotron emission. In the next section we discuss the *Spitzer* observations; we then present our results and discuss their implications.

2. OBSERVATIONS

The IRS on the *Spitzer Space Telescope* has been described by Houck et al. (2004). The IRS provides spectra from 5.2 to 38 μm at resolutions of $R \sim 90$ and 600. The data presented below were all obtained in the low-resolution mode. At low resolution, there are four different observing modes, SL1, SL2, LL1, and LL2, that correspond to four different spectral regions. SL1 uses a 5.84 line mm^{-1} grating (blazed at 11.5 μm) in first order, covering the wavelength region of $7.4 \leq \lambda \leq 14.0$ μm. SL2 uses the same grating in second order, and covers the spectral region $5.2 \leq \lambda \leq 7.7$ μm. A similar grating (5.62 lines mm^{-1} blazed at 31.5 μm) is used in the long-wavelength mode, with LL1 being first-order, covering the wavelength region 19.5–38 μm, and LL2 being second-order, covering the region 14.0–23.0 μm. To change from one mode to another requires offsetting the telescope to a slightly different slit position.

A journal of the observations for our nine program IPs is provided in Table 1, where we list the observation date, the start time of the observations (UT), the observing modes with exposure times and the number of cycles in each mode, the total duration of the observations, the IP orbital period, the spin period of the white dwarf, and the binary orbital inclination. In addition to the IRS data for our nine IPs, we extracted archived IRS observations of AE Aqr (Houck GTO-2 "IRS_DISKS"), and GK Per (Gehrz "RDG-GTO"), two peculiar members of this heterogeneous cataclylsmic variable (CV) subclass. AE Aqr is significantly brighter than any of the other IPs, and excellent spectra were obtained in both short- and long-wavelength modes. In addition to the observations listed in Table 1, AE Aqr was observed for three cycles in the LL1 mode with 100 s exposure times. GK Per was only observed in the SL1 and SL2 modes.

To provide estimated mid-infrared fluxes for planning our observations, we simply used a power-law extrapolation of the optical/IR SED of each target. Surprisingly, these estimations were quite good, falling within 20% of the observed fluxes. Our

TABLE 1
OBSERVATION JOURNAL AND PROGRAM OBJECT CHARACTERISTICS

			Exposure Time						
Object	Observation Date	UT Start	SL1 (s)	SL2 (s)	LL2 (times no. of cycles)	Duration (minutes)	P_{orb} (hr)	P_{spin} (minutes)	i[a] (deg)
V603 Aql	2005 Oct 14	10:41:39	6 × 5	6 × 5	14 × 5	9.5	3.32	61	13
AE Aqr	2004 Nov 13	08:36:52	14 × 2	14 × 2	30 × 3	12.9	9.88	0.55	55
FO Aqr	2005 Nov 23	11:13:52	240 × 2	240 × 3	120 × 5	75.0	4.84	21	65
TV Col	2005 Oct 13	08:59:18	240 × 2	240 × 3	120 × 5	75.0	5.49	32	70
TX Col	2005 Oct 13	07:02:57	240 × 2	240 × 2	120 × 5	67.0	5.72	32	<30
PQ Gem	2006 Apr 23	20:39:48	240 × 2	240 × 2	120 × 4	63.1	5.19	14	60
DQ Her	2005 Oct 19	23:11:49	240 × 2	240 × 3	120 × 5	75.0	4.64	2.4	89.7
EX Hya	2006 Mar 4	01:30:01	60 × 2	60 × 2	120 × 5	32.9	1.64	67	77
GK Per	2004 Mar 1	08:25:07	30 × 2	30 × 2	...	3.0	48.1	6.02	<73
AO Psc	2005 Dec 11	10:04:16	240 × 2	240 × 1	120 × 4	50.1	3.59	13	<30
V1223 Sgr	2006 Apr 17	11:45:43	60 × 5	60 × 5	120 × 5	50.9	3.37	61	13

[a] From Ritter & Kolb (2003).

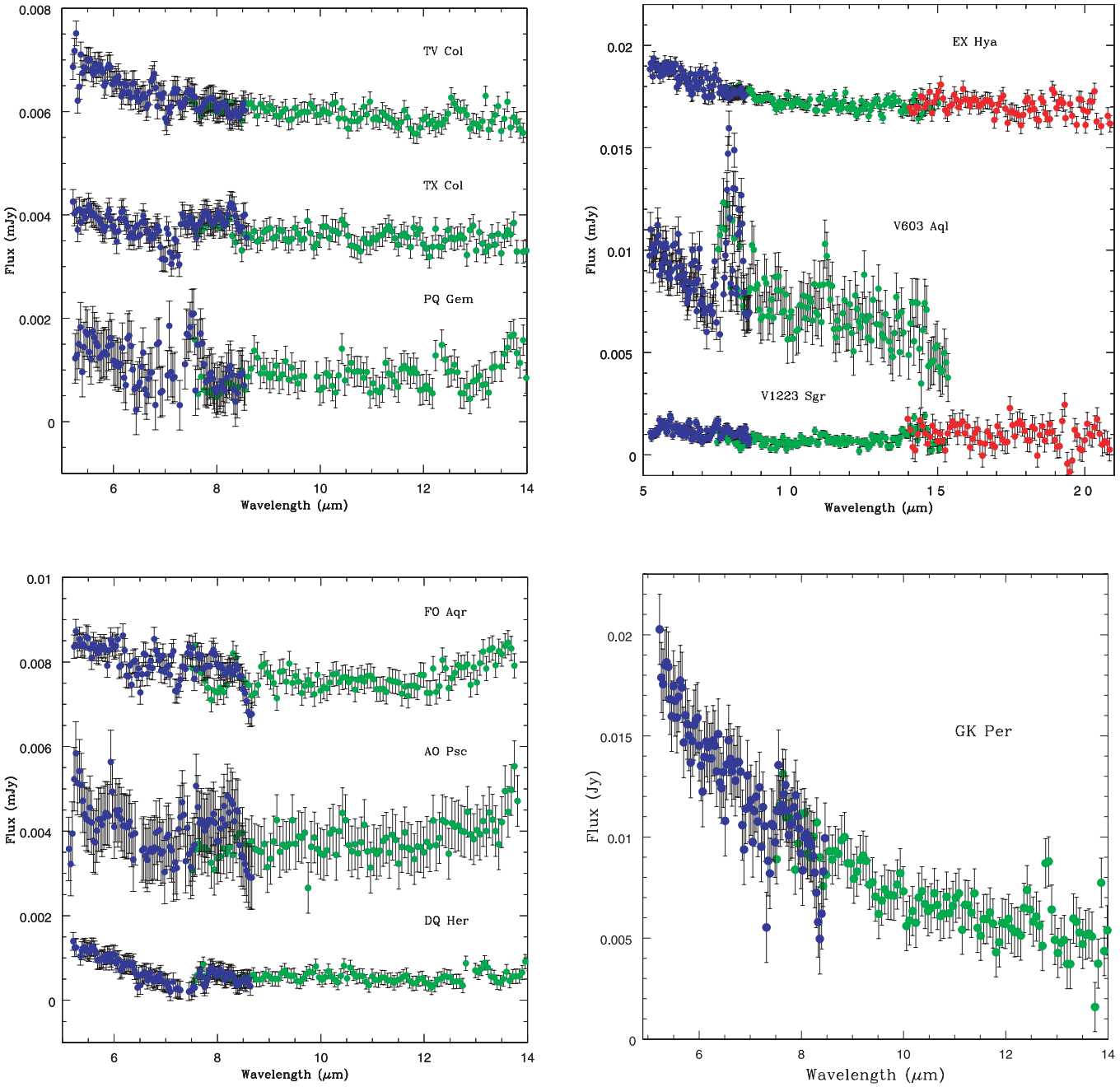

FIG. 2.—IRS spectra of the intermediate polars. (*a*) The spectra of TV Col, TX Col, and PQ Gem. The spectra for TV Col and TX Col have been vertically offset by 0.005 and 0.003 mJy, respectively, for clarity. The spectra have also been color-coded to delineate the different IRS modes: blue is SL2, green is SL1, and red is LL2. (*b*) The data for EX Hya, V603 Aql, and V1223 Sgr. The spectra for EX Hya and V603 Aql have been offset by 0.016 and 0.0035 mJy, respectively. The spectrum of V603 Aql appears to have a strong emission line at 8 μm. (*c*) The data for FO Aqr, AO Psc, and DQ Her. The spectra for FO Aqr and AO Psc have been offset by 0.0068 and 0.003 mJy, respectively. (*d*) The IRS data for GK Per.

goal was to achieve a S/N = 10 in the continuum for each object in the SL1 and SL2 modes. This was not attained for any of our nine sources, however, with a typical signal-to-noise ratio (S/N) near 6. We had hoped for similar quality spectra in the LL2 mode, but only two of the nine target IPs (EX Hya and V1223 Sgr) were detected in the LL2 mode, and both at very low S/N ($\leq$1.5). While this result is somewhat discouraging, note that the hope was to detect cyclotron emission above and beyond that of the accretion disk continuum; thus our results provide useful constraints on any mid-infrared cyclotron emission. Due to the expected faintness of our nine targets, we did not attempt observations of any of our nine IPs in the LL1 mode.

Due to the fact that both of the arrays in the instrument are simultaneously exposed, data on the background are measured in SL1 (LL1) while observing in SL2 (LL2), and vice versa. Thus, while we nodded the program objects along the slit for sky subtraction (a "cycle") in each observing mode, additional sky spectra were automatically obtained from the array, which contained no source spectra. Thus, in some cases (V603 Aql and V1223 Sgr) up to 15 sky spectra were obtained that could be medianed together and subtracted from an object spectrum. Before using the "*Spitzer* IRS Custom Extractor" (SPICE) tool to extract our program object spectra, we used IRAF to median combine all of the sky data, and then subtract these from the program object

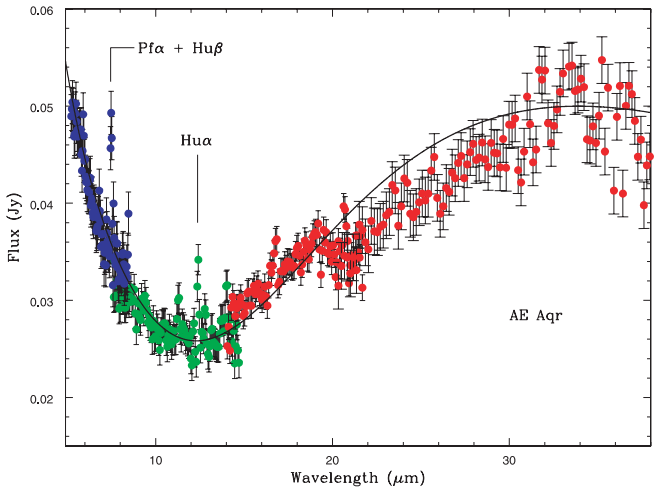

FIG. 3.—IRS spectrum of AE Aqr. While the short-wavelength data are consistent with a power law, at $\lambda > 10$ μm, there is a considerable excess. The solid line in this figure is a power law ($f_\nu \propto \nu^{0.9}$) + blackbody ($T_{\rm eff} = 140$ K) model. Emission lines from the Humprheys α and Pfund α (+Hu β) lines of H I are clearly present.

spectra. This procedure produced a much cleaner sky subtraction than if we had simply subtracted alternating images. The SPICE[2] package extracts and flux calibrates the IRS spectra using both bad pixel masks and other calibration data that come included with your observations. All of our extractions were performed using the standard procedure. The final IRS spectra for 10 of the IPs are shown in Figure 2. The data for AE Aqr are shown in Figure 3. The error bars on the fluxes presented in these figures were determined using IRAF, since SPICE does not properly propagate the various uncertainties through the reduction process. As such, these errors are the means for each spectrum and do not reflect the true uncertainties of any single data point (the errors on the fluxes generally increase with wavelength in both spectral ranges).

In addition to the IRS data just noted, we present near-infrared spectra of the polar EF Eri, and five IPs obtained using SPEX (Rayner et al. 2003) on the IRTF. EF Eri was observed in low-resolution mode ($R \sim 250$) on 2004 August 16. The IPs V603 Aql, AE Aqr, FO Aqr, DQ Her, and GK Per were observed on 2004 August 15. The IPs were observed using the cross-dispersed mode, covering the wavelength interval $0.80 \leq \lambda \leq 2.42$ μm, with a resolution of $R \sim 2000$. Nearby A0 V stars were used for telluric correction, and these data were telluric-corrected and flux- and wavelength-calibrated using the SPEXTOOL package (Vacca et al. 2003). The spectrum of EF Eri is presented in Figure 1, and those for the IPs are presented in Figures 4–8.

3. RESULTS

As shown in Figure 1, the cyclotron harmonics in polars are very broad features that can be easily seen in low-resolution spectra. However, no such features are see in the IRS spectra of *any* of the IPs. While there is structure in the spectra of all of the IPs, we do not believe these are due to cyclotron features. The best case for "optically thin" (see below) cyclotron emission appears to be V603 Aql, with a strong emission feature at 8 μm, but several of the other IPs have "features" or discontinuities in the wavelength region between 7 and 9 μm. There appears to be some type of flaw in the data, or in the reduction process, that has difficulty in this wavelength region for low-S/N data (the data for V603 Aql are quite poor). While we cannot completely dismiss the possibility that these features are real, it will take additional observations to confirm their existence. In addition to the 8 μm region, there is an artifact that produces excess emission at wavelengths near 14 μm in the SL1 mode. As described in the IRS Handbook, this "teardrop" is apparently due to a scattered light problem. The most recent versions (we used version S13) of the pipeline processing greatly reduce the effect, but do not appear to completely eliminate it from the spectra of very faint sources. Thus, any flux excesses beyond 12 μm in the SL1 mode should not be trusted in the data presented here. As shown in Figure 3, AE Aqr has a significant long-wavelength excess, and we treat it separately below.

Given the rather low S/N of the IRS data, we decided to create photometry from these spectra to better examine the spectral energy distributions (SEDs) of these objects for possible mid-infrared excesses. For this process, we created mean flux densities of the sources in 1 μm increments. Because the spectra do not exactly start and stop within perfectly defined wavelength intervals, the fluxes at the endpoints of each mode are not fully 1 μm intervals. For those intervals, we calculated the mean wavelength of the data that was averaged. We have compiled photometry of all of the IPs from published sources, and construct SEDs from the *U* band through 14 μm for eight sources, and through 21 μm for EX Hya and V1223 Sgr. We present these data in Figure 9. Note that the LL2 data at the longest wavelengths for both EX Hya and V1223 Sgr generally have a S/N ≤ 1, and thus are somewhat unreliable, even when averaged.

Given the variable nature of the optical and near-infrared emission from these objects, it is remarkable how well nonsimultaneous data can be fitted with a simple power-law spectrum. The optical/infrared SEDs for V603 Aql, FO Aqr, PQ Gem, AO Psc, TV Col, and V1223 Sgr are easily modeled with power-law spectra ($f_\nu \propto \nu^\alpha$) with indices of $0.8 \leq \alpha \leq 1.3$. Note also that there is no evidence for secondary stars in our IRTF data for V603 Aql, FO Aqr, or DQ Her. The SEDs of TX Col and DQ Her are not as easily fit with power laws, but this could be due to changes in state between the epochs of the optical/near-infrared data and the *Spitzer* observations. The IRS data for both objects are consistent with power-law spectra. The SED for EX Hya suggests that the secondary star is a significant contributor to the near-infrared fluxes, while the SED for GK Per is dominated by its subgiant secondary star in the optical and near-infrared.

It is clear that the dominant source of luminosity in the shorter period IPs is due to their accretion disks. We find that there is no evidence for mid-infrared excesses in these 10 IPs. This is in stark contrast to *Spitzer* mid-infrared (IRAC) photometry of several polars (Howell et al. 2006, Brinkworth et al. 2006). In nearly every polar observed, a significant mid-infrared excess was detected. While the origin for those excesses is unclear, it is possible that a significant fraction of the mid-infrared fluxes in polars can be attributed to cyclotron emission from the lowest harmonics ($n \leq 3.0$).

3.1. *Limits on Cyclotron Emission*

To attempt to place limits on the cyclotron emission in the program IPs, we have generated a large number of models using the one-dimensional cyclotron code first developed by Schwope et al. (1990). This code assumes a constant temperature and plasma "size parameter" (Λ), which is related to the optical depth of the accretion region. We constructed models for field strengths of 0.5, 1, 2, 3, 5, and 7 MG, at two plasma temperatures ($T_{\rm pl} = 10$ and 20 keV), and for two viewing angles ($\Theta = 57^\circ$ and 85°). We

[2] For the SPICE manual go to http://ssc.spitzer.caltech.edu/postbcd/doc/spice.pdf.

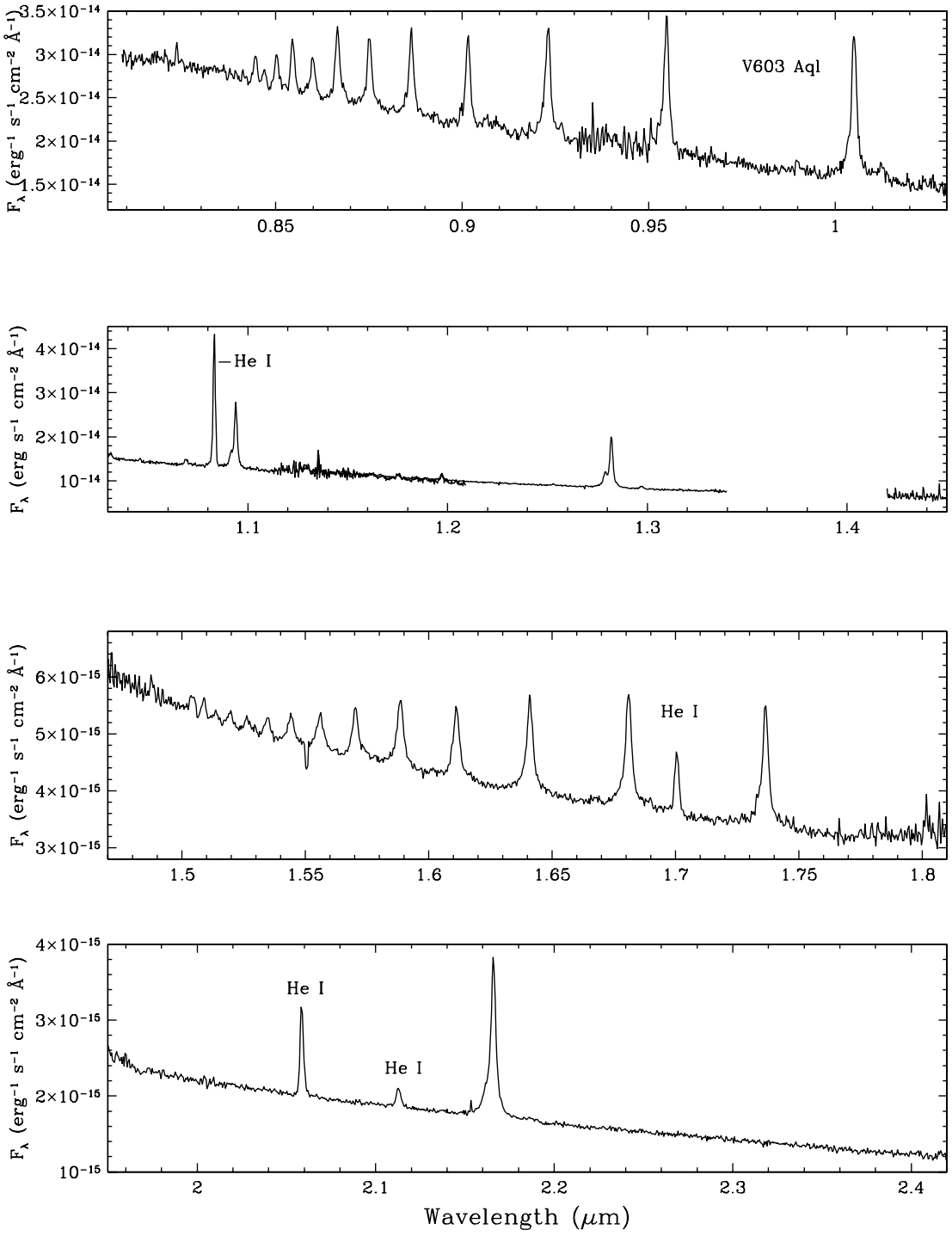

FIG. 4.—IRTF SPEX spectrum of V603 Aql. The spectrum is dominated by emission from the Paschen and Brackett series of H I, and strong He I emission lines (labeled) on a blue continuum. V603 Aql is believed to be a low-inclination system, consistent with the line profiles, although there is a blue asymmetry on some of the stronger lines. There is no evidence for the presence of a secondary star in these data.

ran models that covered a large range in the size parameter: $-5.0 \leq \log(\Lambda) \leq 7.0$. For the discussion below, we refer to models with $\log(\Lambda) \leq 1.0$ to be optically thin, models with $1.0 < \log(\Lambda) < 5$ to be of "intermediate" optical depth, and models with $\log(\Lambda) \geq 5.0$ to be optically thick. A run of these models over a large range in optical depth for a 3 MG field is shown in Figure 10*a*. Note that as the optical depth increases, the discrete cyclotron harmonics merge together to form a continuum. To derive constraints on the possible contribution of the cyclotron emission we combined these models with simple power-law spectra that best fit the optical to mid-IR data for each object. Figures 10*b* and 10*c* show an example of the fitting procedure for EX Hya. Obviously, it is difficult to place tight limits on the contribution of the cyclotron flux given the quality of the IRS spectra and the possibility that the cyclotron emission is optically thick. As shown in Figures 10*b* and 10*c*, it is easy to rule out cyclotron emission for plasmas with $\log(\Lambda) \leq 1.0$, for field strengths between 3 and 7 MG in *all* of our sources to very stringent limits: $\leq$20% of the continuum at the $n = 3$ ($B \geq 4$ MG) or the $n = 4$ ($B < 4$ MG) harmonic (selecting the harmonic that fell closest to

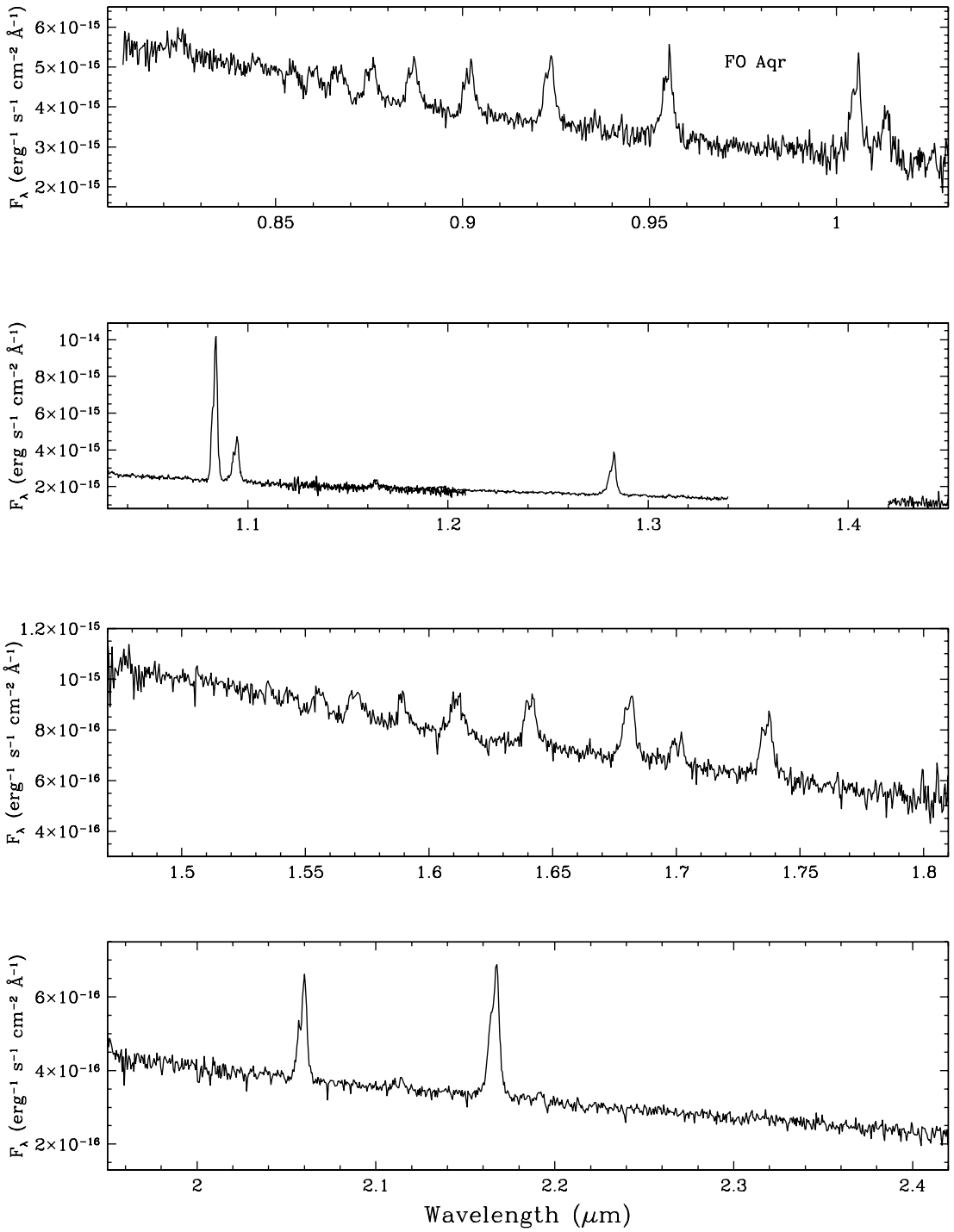

FIG. 5.—SPEX data for FO Aqr. The He I lines (e.g., that at 1.0830 μm) are weaker than those in the spectrum of V603 Aql, and the line profiles are doubled, consistent with an orbital inclination of $i = 65^\circ$.

the center of the SL1 + SL2 bandpasses). At field strengths outside this range, the most prominent cyclotron humps fall outside the bandpasses of the data presented here. However, field strengths larger than 7 MG have harmonics that are located in the near-infrared. If optically thin cyclotron emission was present, we would have clearly detected it in our SPEX data for the five IPs surveyed. Thus, if the cyclotron emission from IPs is optically thin, it must arise from field strengths of $B < 3$ MG.

As the optical depth of the cyclotron region increases, its affect on the continuum becomes increasingly difficult to separate from a power-law spectrum (see Fig. 10*a*). Thus, even for the data with the highest S/N (e.g., EX Hya), we cannot rule out contributions of up to 50% for optically thick cyclotron emission. For those objects with lower S/N data, we cannot rule out the possibility that their mid-infrared spectra are dominated by optically thick cyclotron emission. Even with such limits, however, it is important to realize that this is a significant constraint. For example, in polars, the optical/IR cyclotron emission can be a considerable fraction of their bolometric luminosities. While IPs have a strong accretion disk component that polars do not, the contrast between the cyclotron emission and the local accretion disk flux increases with increasing wavelength, due to

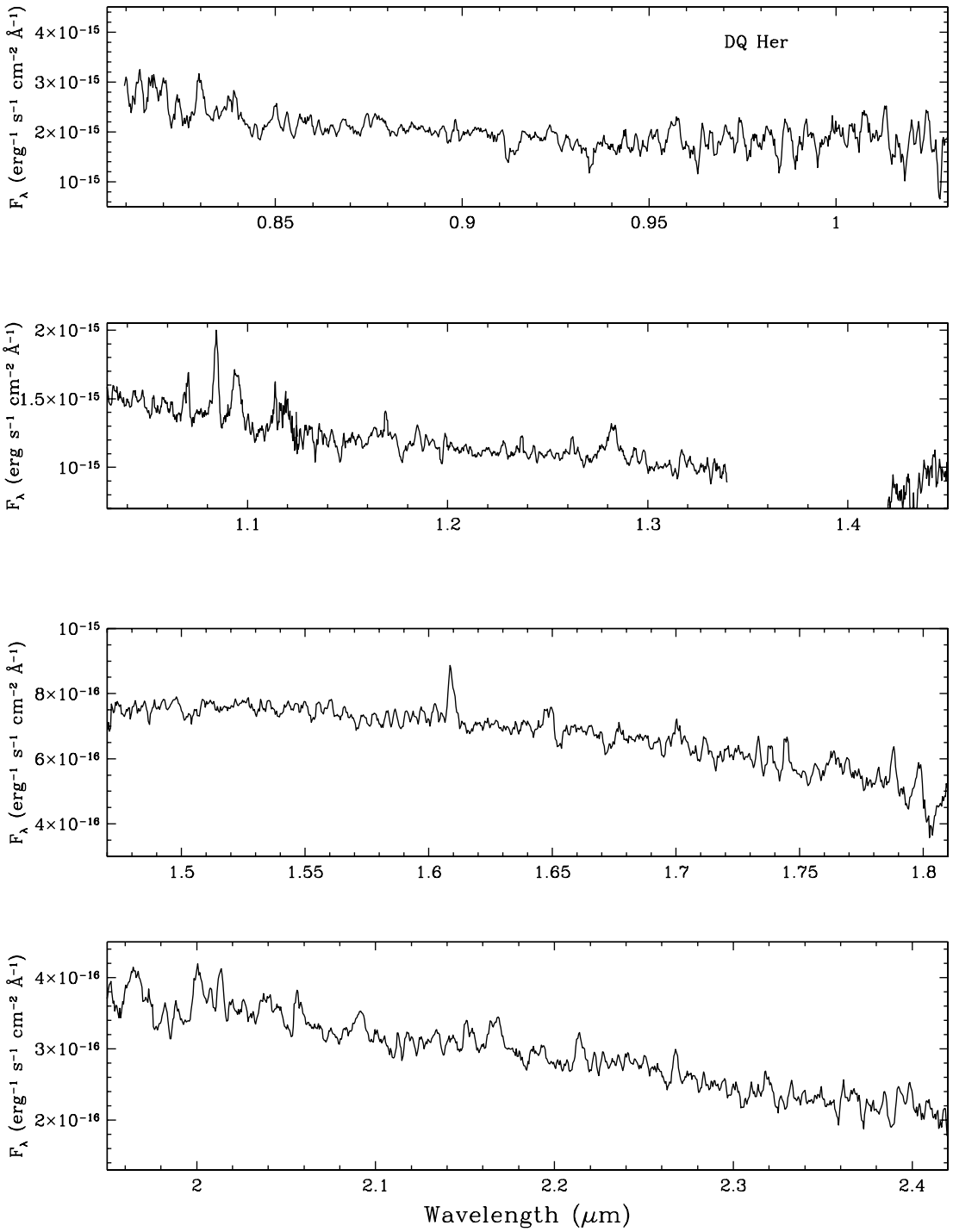

FIG. 6.—IRTF spectrum of DQ Her. DQ Her is a faint source, $K \sim 13.1$, and a challenging target at this spectral resolution. Thus, the data have substantially lower S/N, and the spectrum shown here was boxcar smoothed by a factor of 5. The H I and He I lines are broader than the previous two objects, consistent with DQ Her's edge-on inclination ($i = 89.7^\circ$).

fact that the peak of the cyclotron emission for low strength fields falls in the IRS bandpasses, while the accretion disk spectrum is declining. We conclude that any contribution from optically thick cyclotron emission in the wavelength interval $5.2 \leq \lambda \leq 14$ μm is <0.5% of the bolometric luminosities of the program IPs.

V1223 Sgr, and to a lesser extent, EX Hya, both show excesses in the LL2 bandpass (Fig. 9*b*). While these spectra are quite poor, most of the photometric fluxes in this spectral region have S/N > 3. As discussed for AE Aqr, below, we can model excesses in this wavelength range with cyclotron emission from fields with $1 \leq B \leq 2$ MG. The final model for AE Aqr, derived below, fits the data for both EX Hya and V1223 Sgr reasonably well. Given the similarity between the long-wavelength excess in V1223 Sgr and AE Aqr, it would be useful to obtain higher quality LL2 and new LL1 spectra of both V1223 Sgr and EX Hya to conclusively determine the reality of their apparent excesses.

3.2. *The Mid-Infrared Excess of AE Aqr*

In contrast to the results above, is the spectrum of AE Aqr. AE Aqr is a peculiar object. The white dwarf in AE Aqr spins

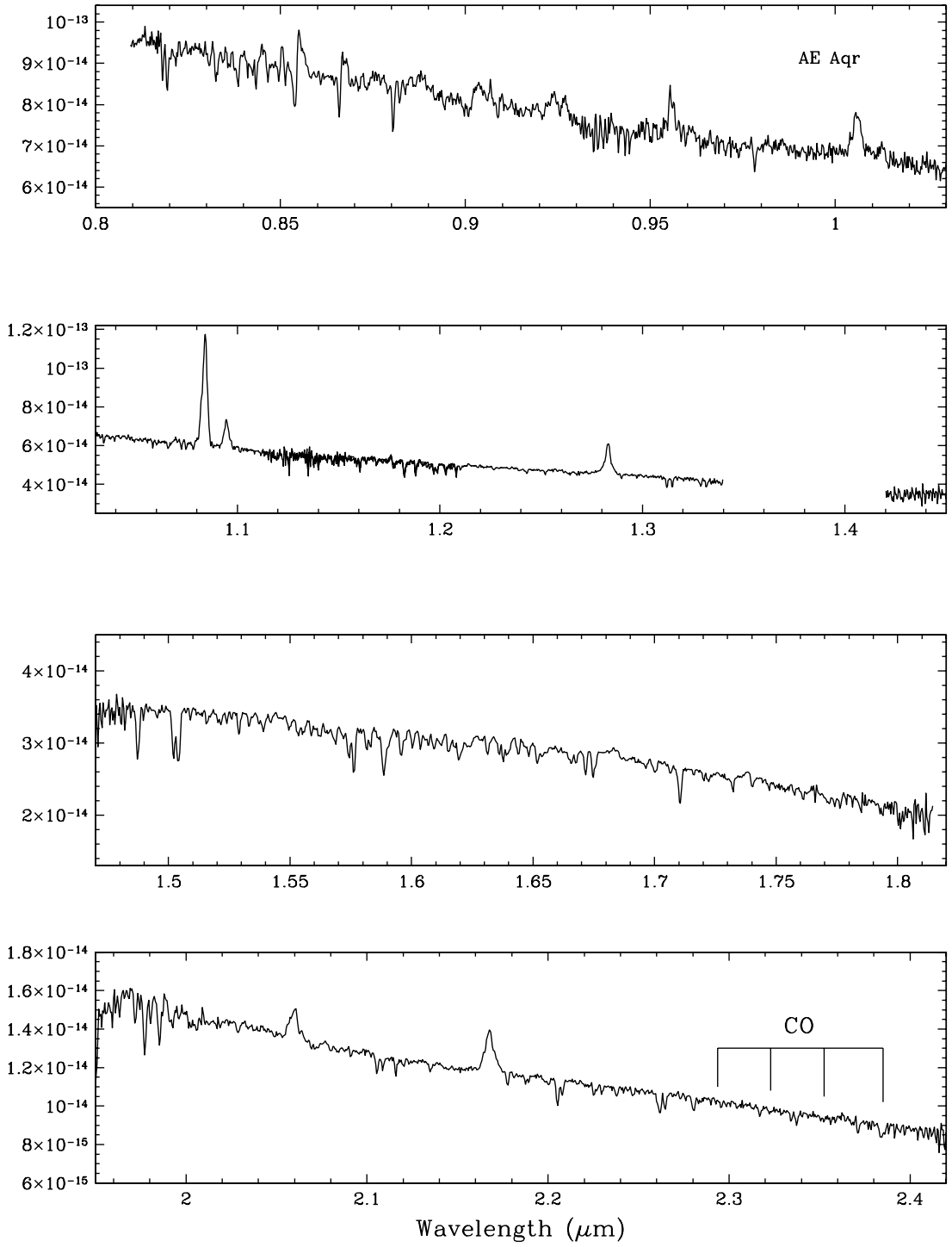

FIG. 7.—SPEX data for AE Aqr are dominated by the secondary star—even the Na I doublet at 0.82 μm is clearly visible. The atomic absorption features are consistent with a spectral type of K4, except that such an object should have strong CO absorption features. There is no evidence for ^{12}CO absorption (positions for the main band heads indicated) in this spectrum, suggesting that carbon is highly deficient (the absorption feature at 2.38 μm is actually a doublet of Mg I).

faster than any other (33 s), but this rotation rate is also rapidly slowing, at a rate of 6×10^{-14} s s^{-1} (De Jager et al. 1994), the most rapid spin-down rate known. This rapid spin down cannot be explained by normal accretion torques, and thus a "magnetic propeller" model (Wynn et al. 1997) has been developed where the spinning magnetic field of the white dwarf ejects material from the system. It has been suggested by Schenker et al. (2002) that AE Aqr is a brand new CV, having just emerged from the common envelope phase. UV spectra of AE Aqr reveal an extreme N V/C IV ratio, suggesting a deficit of carbon and an enhancement of nitrogen. This indicates that material that has been processed through the CNO cycle is making its way to the surface of the white dwarf primary. The near-infrared spectrum of AE Aqr is consistent with these results, revealing a late-type (K4) secondary star, *but one that has no evidence for* ^{12}CO *absorption features*! This implies a secondary star that is highly deficient in carbon, a general result found for many CVs (see Harrison et al. 2004b, 2005b), but AE Aqr and GK Per are the

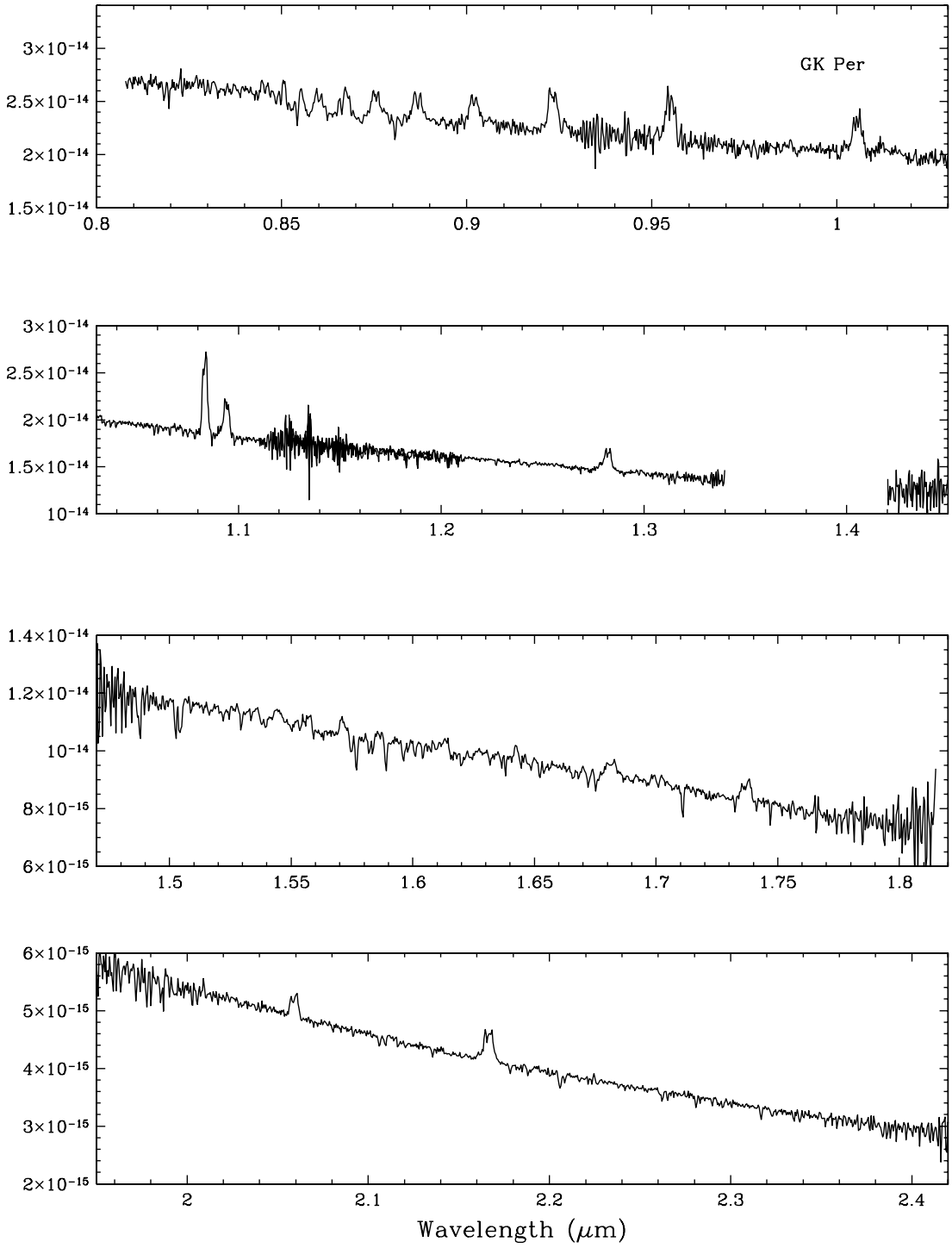

FIG. 8.— IRTF spectrum of GK Per is also dominated by its late-type subgiant secondary star. As discussed by Harrison et al. (2005a), nearly all of the atomic absorption features in the spectrum of GK Per are weaker than they should be, suggesting a subsolar metallicity for the secondary star.

most extreme cases we have found in our infrared spectroscopic surveys.

The IRS spectrum of AE Aqr is shown in Figure 3. Shortward of 12 μm, the spectrum is consistent with a power law, but beyond this wavelength there is a considerable flattening of the spectrum. The SED of AE Aqr, including the IRS data, is plotted in Figure 11. In addition to the IRS data, we plot point source fluxes from *IRAS* at 25 and 60 μm, and ground-based observations at M', 11.7 and at 17.6 μm from Dubus et al. (2004). Dubus et al. reported that these fluxes were highly variable. If we ignore the IRS data, the 17–60 μm fluxes of AE Aqr can be fitted with a cool blackbody ($T_{\rm BB} = 125$ K). The IRS data (see Fig. 3), can also be fit with a blackbody, but one with a slightly higher temperature: $T_{\rm BB} = 140$ K. Given the likelihood of matter being ejected from the binary system, a circumstellar dust shell around AE Aqr is not unexpected. Assuming black grains, this dust intercepts about 1% of the bolometric flux from AE Aqr.

Given the evidence for short-timescale variability, a circumstellar dust shell is probably not the best explanation for the mid-infrared excess of AE Aqr. Dubus et al. (2004) discuss the

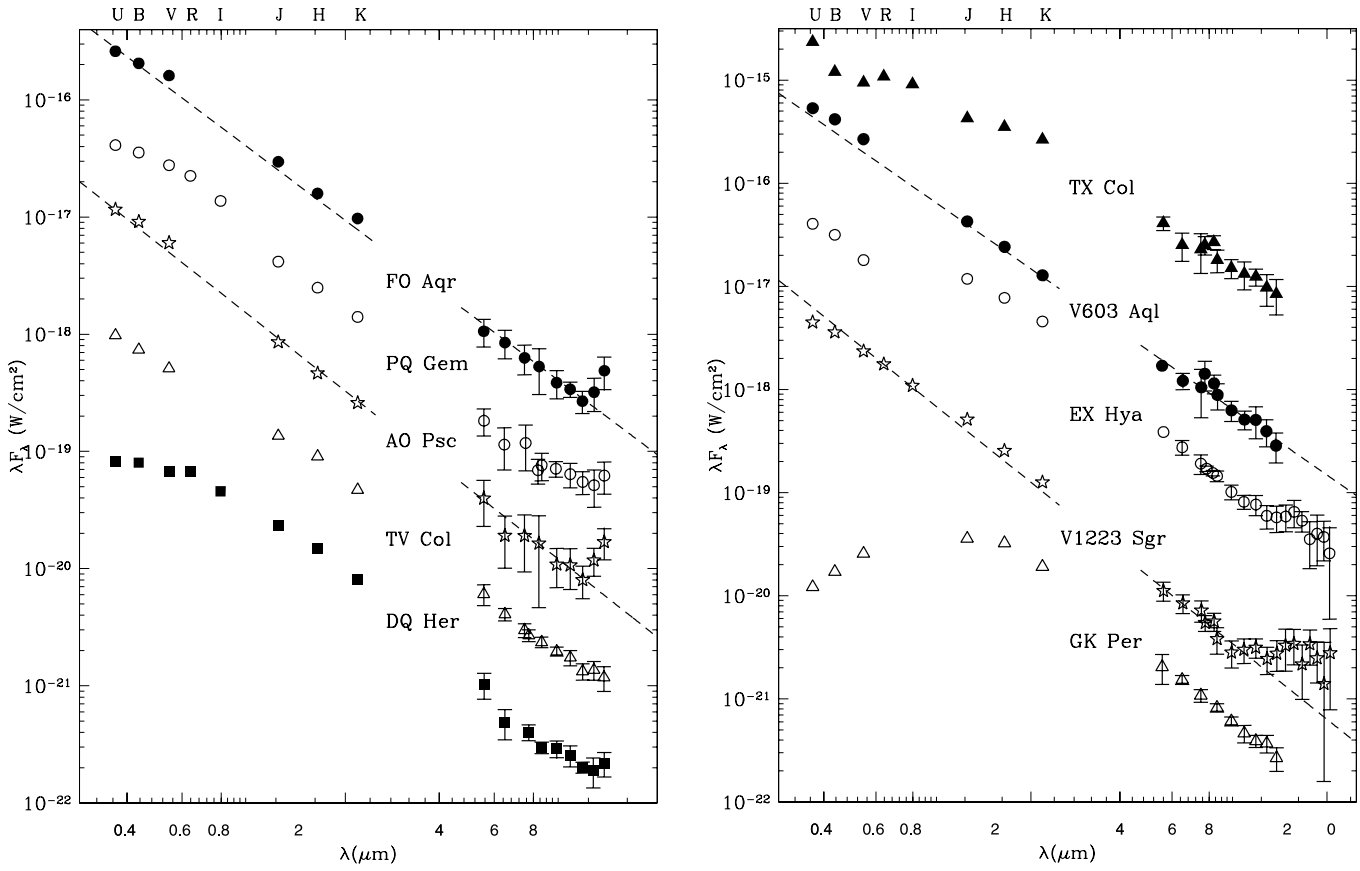

FIG. 9.—(*a*) The optical to mid-infrared SEDs for the program objects (*JHK* photometry from Hoard et al. [2002], unless otherwise noted): FO Aqr (*filled circles*, *UBVJHK* from Szkody 1987), PQ Gem (*open circles*, *UBVRI* from Potter et al. 1997), AO Psc (*stars*, *UBV* from Bruch & Engel 1994), TV Col (*triangles*, *UBV* from Bruch & Engel 1994), and DQ Her (*squares*, *UBVRI* from Schoembs & Rehban 1989). Each of the SEDs has been offset for clarity. Power-law spectra (*dashed lines*) have been fitted to the SEDs of FO Aqr ($f_\nu \propto \nu^{1.0}$) and AO Psc ($f_\nu \propto \nu^{1.1}$). (*b*) the SEDs for TX Col (*solid triangles*, *UBVRIJHK* from Buckley & Touhy 1989), V603 Aql (*filled circles*, *UBV* from Bruch & Engel 1994), EX Hya (*open circles*, *UBV* from Vogt 1983), V1223 Sgr (*stars*, *UBVRI* from Bonnet-Bidaud et al. 1982), and GK Per (*triangles*, *UBVJHK* from Sherrington & Jameson 1983). Power laws have been fit to the SEDs of V603 Aql ($f_\nu \propto \nu^{1.0}$) and V1223 Sgr ($f_\nu \propto \nu^{1.3}$). The SED of EX Hya shows a near-infrared excess, which is probably due to its late-type secondary star. The SED of GK Per is dominated by its secondary star. Both V1223 Sgr and EX Hya appear to have a long-wavelength excess. Error bars are plotted when larger than the symbol size.

possibility of explaining their observations with synchrotron radiation, a mechanism consistent with both the mid-infrared and radio properties of this source. In addition, AE Aqr has been detected at TeV energies (Meintjes et al. 1992)! The fact that there is no apparent turnover in the slope of the spectrum shown in Figure 3 suggests that the transition from optically thin to thick synchrotron emission occurs at wavelengths longer than 38 μm (see Dubus et al. 2004). Here, however, we explore the possibility that the observed mid-infrared excess is due to cyclotron emission, a process that can also explain the rapid variability of

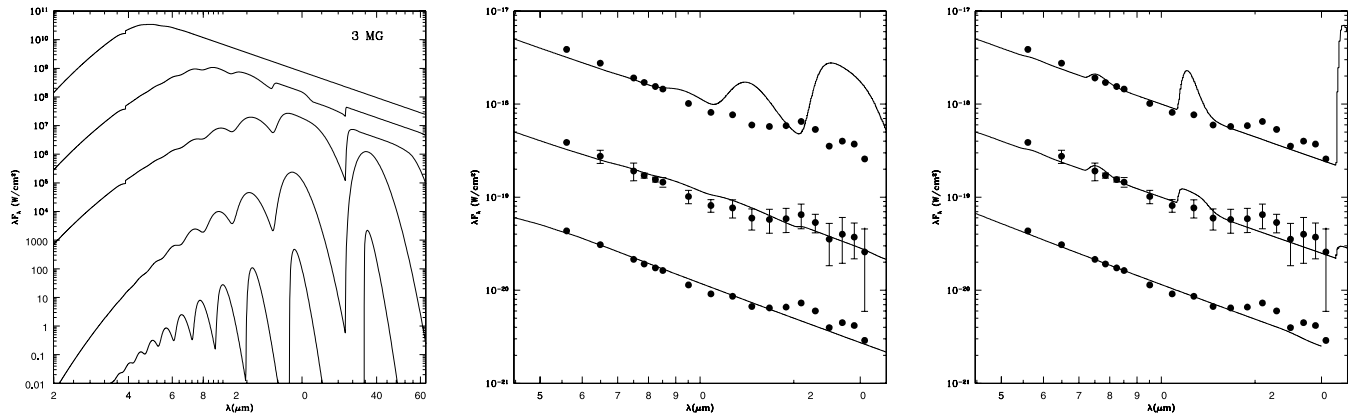

FIG. 10.—(*a*) Model cyclotron spectra for a 3 MG field with a plasma temperature of $T_{\rm pl} = 20$ keV, a viewing angle of $\Theta = 57^\circ$, and for a large range of (*from top to bottom*) $\log(\Lambda) = 5.0, 3.0, 1.0, -3.0$, and -5.0. As the optical depth is increased, the discrete cyclotron harmonics ($n = 1$ is the rightmost) are replaced with a nearly featureless continuum. (*b*) Cyclotron + power-law models fit to the IRS data for EX Hya. Error bars are plotted for the middle SED. The cylotron models shown here have $B = 3$ MG, $T_{\rm pl} = 20$ keV, $\Theta = 57^\circ$, and $\log(\Lambda) = 1.0$, 3.0, and 5.0. The cyclotron models were normalized so that the peak of the $n = 4$ harmonic, located at 9 μm, accounts for 20% of the power-law flux at this wavelength. (*c*) The same, but for a field strength of 5 MG. The cyclotron spectra were normalized so that the peak of the $n = 3$ harmonic at 7.6 μm accounts for 20% of the power-law flux at this wavelength.

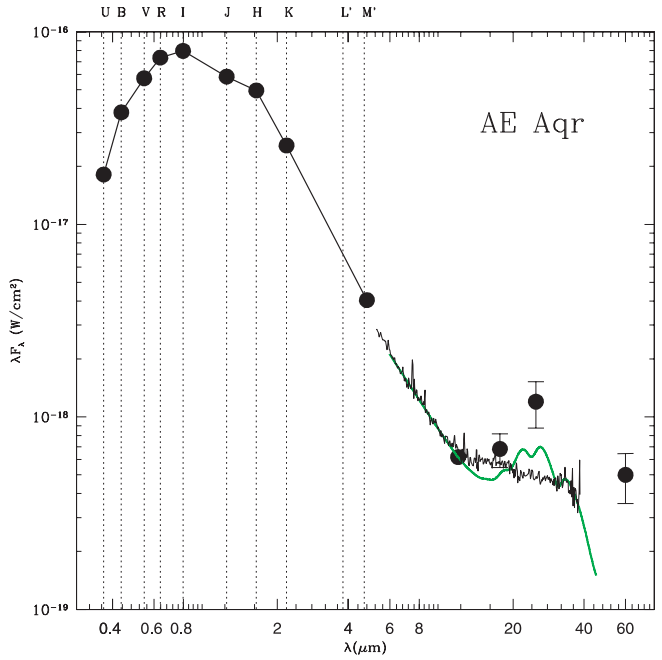

FIG. 11.— SED of AE Aqr. The optical/near-infrared fluxes of AE Aqr are dominated by its secondary star. *UBVRIJHKL′M′*, 11.7 and 17.6 μm fluxes are from Dubus et al. (2004), while the 25 and 60 μm fluxes are from *IRAS*. The IRS spectrum is the thin line, and a power law ($f_\nu \propto \nu^{0.9}$) + cyclotron model ($B = 1$ MG, $T_{\rm pl} = 20$ keV, $\Theta = 57^\circ$, and $\log(\Lambda) = 3.0$) is shown as the heavy green line.

this source. It is clear that well-defined, discrete cyclotron harmonics are not present in the IRS data for AE Aqr, suggesting that any cyclotron emission must be optically thick. Our models indicate that the magnetic field strength cannot be much higher than 1 MG, as the excess would occur at shorter wavelengths. As the optical depth of the cyclotron emission region is increased, the maximum emission shifts away from the lower harmonics (and their longer wavelengths), forming a psuedocontinuum in the higher harmonics at shorter wavelengths. For completely optically thick emission at a field strength of 1 MG, the peak in the cyclotron flux occurs near 10 μm. To provide the observed infrared excess requires emission from a region of intermediate optical depth, and such would have discrete harmonics in the observed bandpass. While we have not explored the entire parameter space, we find that the best-fitting model has $B = 1$ MG and is of intermediate optical depth (Fig. 11). None of our models could create a featureless excess that is as broad as that which is observed. Clearly, the blackbody fit does a better job, and we therefore believe that this excess is probably not due to cyclotron emission.

4. DISCUSSION

While there is no a priori expectation that the magnetically controlled accretion in IPs is similar to that in polars, their X-ray properties, and the detection of circular polarization in some IPs argues that they share some commonality. Thus, the complete lack of detectable cyclotron emission in these IPs is puzzling. There are a number of possible explanations: (1) cyclotron emission is only emitted during a small fraction of a spin/orbital period, or does not occur along our line of sight; (2) the properties of the IPs examined here are such that cyclotron emission is unimportant; or (3) the magnetic field strengths of IPs are higher or lower than currently believed. We examine each of these scenarios below.

Cyclotron emission from most polars *is* only visible during part of an orbit. For some polars, there are times during an orbital period where the cyclotron emission disappears, or at least becomes insignificant compared to other sources in the system. In other cases, such as EF Eri (see Harrison et al. 2004a), cyclotron emission apparently dominates throughout an orbital period. It could be that the field geometry of the IPs is such that the cyclotron emission is only present for a brief interval, and that our short-duration observations were insufficient to catch the cyclotron maximum. But this seems to be the least likely explanation. If the cyclotron emission in IPs occurs near the magnetic poles of the white dwarf, then given that the white dwarf primaries in these systems are spinning much more rapidly than their orbital periods (see Table 1), our observations were of sufficient length to have fully covered the spin periods for most of our sources. However, if the cyclotron emission occurs only for a brief interval during a spin period, it could be highly diluted in cases where the spin period is very short (e.g., AE Aqr or DQ Her) relative to the exposure times of our observations. Examination of the individual spectra for all of the IPs shows no significant changes from one spectrum to the next, however, ruling this out for those sources with complete spin phase coverage.

Even if the cyclotron emission was somehow tied to the orbital period, the cyclotron emission is visible for $\gtrsim$20% of an orbit in polars, and given that we have data for 11 sources, the chances that this emission was missed in all of them would be hard to accept. The 11 IPs observed by *Spitzer* also cover a wide range in orbital inclination, from the eclipsing system DQ Her to the nearly face-on system V603 Aql. It seems unlikely that beaming affects are the explanation for our nondetection of cyclotron emission.

Discrete cyclotron harmonics are usually only seen during periods of low-mass accretion in polars ("low states"). In polar "high states" these features generally disappear and are replaced by a strong accretion continuum. It is likely that the accretion rate in IPs is always equivalent to, or greater than that found in polar high states, and thus emission from discrete cyclotron harmonics is suppressed. But much of the emission from polars during high states *is* due to cyclotron emission, that from optically thick cyclotron emission. Examination of the SEDs of polars in and out of high states reveals that they derive much of their luminosity from optically thick cyclotron emission. For example, both AM Her (Bailey & Axon 1981) and EF Eri (Bailey et al. 1982) in their high states emit strongly circularly polarized radiation. In the case of EF Eri, discrete cyclotron harmonics are even present *during* a high state (Ferrario et al. 1996). Thus, while it seems likely that discrete harmonics might never be detected from IPs, optically thick cyclotron emission might occur. As detailed above, such emission would have been visible if it constituted more than $\sim$50% of the local continuum.

Woelk & Beuermann (1996) note that for field strengths of $B \sim 5$ MG and very high accretion rates, $m \geq 1$ g cm^{-2} s^{-1}, cyclotron cooling becomes insignificant, and free-free radiation dominates. Mass accretion rates for IPs are in this range (Buckley & Tuohy 1989, Wu et al. 1989, Bonnet-Bidaud et al. 1982), depending on the choice for the size of the accretion column footprint. Optically thin free-free radiation has a spectrum of $f_\nu =$ constant, however, and all of our spectra have power-law indices that decline much more rapidly than this. Thus, as in our arguments about optically thick cyclotron emission, the mid-infrared spectra show little evidence for significant free-free emission.

The similarity of the excesses in EX Hya and V1223 Sgr to that of AE Aqr begs the question whether synchrotron emission is the dominant cooling process in all IPs. It should be possible to obtain adequate spectra with the IRS for several of the systems that we have observed here, using longer effective exposure times to test this idea. It is interesting to note that both BG CMi and DQ Her have been detected as flaring radio sources (Pavelin

et al. 1994). Perhaps a deeper survey of IPs at radio wavelengths might be warranted.

It could be that the actual field strengths for IPs lie outside the range which would produce cyclotron emission at the mid-infrared wavelengths we have surveyed. Sensitive searches at both visual and near-infrared wavelengths have failed to reveal any sign of discrete cyclotron humps. The SEDs shown in Figure 9 confirm this result. Thus, there are strong constraints on optically thin cyclotron emission at optical, near-infrared, and mid-infrared wavelengths. In a low-resolution infrared spectroscopic survey of polars, R. K. Campbell (2007, in preparation) found that rarely is there discrete cyclotron emission at harmonics above $n = 6$, and only occasionally is there significant emission at harmonics with $n \leq 2$. Assuming that this is true for IPs, is it possible for such emission to have escaped detection in the window between 2.3 and 5.5 μm? For field strengths between 7 and 9 MG, harmonics 3–6 would mostly occur in this unobserved bandpass, or within the water vapor features found in the near-infrared. Given the possibility of optically thick emission, it seems likely that it would be easily overlooked. Thus, the field strengths for the program IPs could all fall within this narrow range. Such a proposition could be easily tested by obtaining phase-resolved *L*- and *M*-band photometry for a number of systems.

Alternatively, the magnetic field strengths could all be significantly higher or lower than previously expected. For field strengths above 100 MG, the cyclotron emission would mostly occur in the UV, and could be easily missed if dominated by the emission from the accretion disk. But if the magnetic fields of the white dwarfs were this large, it would be hard to explain why these objects are not synchronously rotating. We certainly cannot rule out lower field strengths. For field strengths of $B \leq 1$ MG, very little cyclotron emission would fall within the IRS bandpass, and thus, could have been missed for the 11 IPs surveyed. Our models for V1223 Sgr and EX Hya suggest the possibility of fields near 1 MG in those two sources. It appears that if the primary stars in IPs are magnetic, it is likely that their field strengths are low, $B \leq 1$ MG.

5. CONCLUSIONS

We have presented a mid-infrared spectroscopic survey of 11 IPs, and present near-infrared spectra for five of these systems. We find that, in general, the mid-infrared spectra of IPs are consistent with the extension of a simple power law from the optical to the mid-infrared. We rule out the presence of optically thin cyclotron emission to very stringent limits and show that optically thick cyclotron emission is an insignificant fraction of the bolometric luminosity if it is occurring within the IRS bandpass. We conclude that the best explanation for our results is that the magnetic field strengths of the white dwarf primaries in intermediate polars are $B \leq 1$ MG, although we cannot rule out high accretion rate scenarios where the cyclotron emission is a small fraction of the total luminosity. We do report a mid-infrared excess for AE Aqr. It is likely, however, that this excess is due to synchrotron radiation.

This work is based in part on observations made with the *Spitzer Space Telescope*, which is operated by the Jet Propulsion Laboratory, California Institute of Technology under a contract with NASA. Support for this work was provided by NASA through an award issued by JPL/Caltech.

REFERENCES

Bailey, J., & Axon, D. J. 1981, MNRAS, 194, 187
Bailey, J., Hough, J. H., Axon, D. J., Gatley, I., Lee, T. J., Szkody, P., Stokes, G, & Berriman, G. 1982, MNRAS, 199, 801
Bonnet-Bidaud, J. M., Mouchet, M., & Motch, C. 1982, A&A, 112, 355
Brinkworth, C. S., et al. 2006, AJ, submitted
Bruch, A., & Engel, A. 1994, A&AS, 104, 79
Buckley, D. A. H., & Touhy, I. R. 1989, MNRAS, 344, 376
De Jager, O. C., Meintjes, P. J., O'Donoghue, D., & Robinson, E. L. 1994, MNRAS, 267, 577
Dubus, G., Campbell, R., Kern, B., Tamm, R. E., & Spruit, H. C. 2004, MNRAS, 349, 869
Ferrario, L., Bailey, J., & Wickramasinghe, D. 1996, MNRAS, 282, 218
Harrison, T. E., Howell, S. B., & Johnson, J. J. 2005a, BAAS, 37, 1276
Harrison, T. E., Howell, S. B., Szkody, P., Homeier, D., Johnson, J. J., & Osborne, H. L. 2004a, ApJ, 614, 947
Harrison, T. E., Osborne, H. L., & Howell, S. B. 2004b, AJ, 127, 3493
———. 2005b, AJ, 129, 2400
Hoard, D. W., Wachter, S., Clark, L. L., & Bowers, T. P. 2002, ApJ, 565, 511
Houck, J. R., et al. 2004, ApJS, 154, 18
Howell, S. B., et al. 2006, ApJ, 646, L65
Meintjes, P. J., Raubenheimer, B. C., de Jager, O. C., Brink, C., Nel, H. I., North, A. R., van Urk, G., & Visser, B. 1992, ApJ, 401, 325
Norton, A. J., Haswell, C. A., & Wynn, G. A. 2004a, A&A, 419, 1025
Norton, A. J., Wynn, G. A., & Somerscales, R. V. 2004b, ApJ, 614, 349
Pavelin, P. E., Spencer, R. E., & Davis, R. J. 1994, MNRAS, 269, 779
Potter, S. B., Cropper, M., Mason, K. O., Hough, J. H., & Bailey, J. A. 1997, MNRAS, 285, 82
Rayner, J. T., Toomey, D. W., Onaka, P. M., Denault, A. J., Stahlberger, W. E., Ritter, H., & Kolb, U., Vacca, W. D., Cushing, M. C., & Wang, S.2003, A&A, 404, 301
Ritter, H., & Kolb, U. 2003, A&A, 404, 301
Schenker, K., King, A. R., Kolb, U., Wynn, G. A., & Zhang, Z. 2002, MNRAS, 337, 1105
Schoembs, R., & Rehban, H. 1989, A&A, 224, 42
Schwope, A. D., Beuermann, K., & Thomas, H.-C. 1990, A&A, 230, 120
Sherrington, M. R., & Jameson, R. F. 1983, MNRAS, 205, 265
Szkody, P. 1987, ApJS, 63, 685
Vacca, W. D., Cushing, M. C., & Rayner, J. T. 2003, PASP, 115, 389
van Amerongen, S., Augusteijn, T., & van Paradijs, J. 1987, MNRAS, 228, 377
van Amerongen, S., Kraakman, H., Damen, E., Tjemkes, S., & van Paradijs, J. 1985, MNRAS, 215, 45
Vogt, N. 1983, A&AS, 53, 21
Warner, B. 1995, Cataclysmic Variable Stars (Cambridge: Cambridge Univ. Press), 367
Wickramasinghe, D. T., Wu, K., & Ferrario, L. 1991, MNRAS, 249, 460
Woelk, U., & Beuermann, K. 1996, A&A, 306, 232
Wu, C.-C., Panek, R. J., Holm, A. V., Raymond, J. C., Hartman, L. W., & Shank, J. H. 1989, ApJ, 339, 433
Wynn, G. A., King, A. R., & Horne, K. 1997, MNRAS, 286, 436